Applicability of Laser Polishing on Inconel 738 Surfaces Fabricated Through Direct Laser Deposition

Srdjan Cvijanovic[1,2], Evgueni V. Bordatchev[*2,1], and O. Remus Tutunea-Fatan[*1,2]

[1]*Mechanical and Materials Engineering, Western University, London, Ontario, Canada*
[2]*Automotice and Surface Transportation Research Center, National Research Council of Canada, London, Ontario, Canada*
[*]*Corresponding author's e-mail: evgueni.bordatchev@nrc-cnrc.gc.ca, rtutunea@eng.uwo.ca*

Today's manufacturing industry requires novel technologies capable to improve process versatility, rapidity as well as the surface quality of the parts fabricated through additive manufacturing. A cost/process-effective manufacturing solution capable to meet these requirements is represented by the direct laser deposition (DLD) technology. DLD is essentially an additive manufacturing (AM) process that can accurately fabricate complex freeform geometries. The main drawback of DLD is constituted by the reduced surface quality that is in fact an unavoidable characteristic of the AM processes. It was found that the best areal surface roughness (*Sa*) occurs on the front wall characterized by a +90° angle (or clockwise rotation) between DLD feed and flow vectors. More specifically, while the front wall is characterize by *Sa* = 0.704μm, the rear/back wall (-90° or counterclockwise rotation) is characterized by *Sa* = 3.861μm because powder is distributed and affixed in an already solidifying molten pool. To counteract this DLD process inconsistency, high-speed laser polishing (LP) can be used as a post processing technique capable to significantly improve the post-DLD surface quality. Along these lines, LP can eliminate and/or reduce the time and the cost of post-DLD surface finishing operations. Preliminary experimental results demonstrate that LP improves the quality of DLD-generated surfaces by decreasing with up to 70% the surface roughness ($S_{a\ LP(90deg)}$ = 0.211 μm, $S_{a\ LP(-90deg)}$ = 0.444 μm) through a redistribution of melted micro-peaks into micro-valleys. The combination of these two laser-based technologies offers an economic, ergonomic, and ecologic fabrication option and opens up avenues for future implementations of computer-based adaptive control, self-optimization, and online monitoring techniques.

DOI: 10.2961/jlmn.2023.01.2002
Keywords: additive manufacturing, direct laser deposition, laser polishing, surface quality

1. Introduction

Presently, a strong desire exists to expedite the fabrication of parts while preserving their high surface finish. In this regard, the use of the additive manufacturing (AM) or 3D printing technologies constitutes a plausible solution for rapid tool-free manufacturing of complex freeform parts. Nonetheless, in most of these cases, a secondary operation is needed to improve the poor surface finish that can significantly affect part properties such as: fatigue strength, material strength and corrosion resistance [1]. An example of AM process used to create metallic parts is represented by direct laser deposition (DLD), a process that generates parts with poor surface roughness (S_a) typically ranging from 5 um to 20 um. This happens due to stair-step structured surfaces, droplet formation, adverse residual stresses, and low dimensional precision and accuracy [1]. Therefore, the main technical challenge resides in that AM components require a finishing operation (manual abrasive polishing, machining, etc.) in order to meet the required surface characteristics and functionality and to improve the material properties that are affected by poor surface quality. Furthermore, the manual polishing process entails advanced technical skills and since it happens at slow rates (~30 min/cm^2 on a flat surface) it leads to high production costs. Finishing by milling will inevitably produce scallops, ridges, and valleys such that irrespective of the trajectory of the cutting tool, the machined surface will always exhibit a degree of form error, waviness, and surface roughness.

Laser polishing (LP) is one of the advanced surface finishing techniques that has been continuously developed over the past two decades [2-6] for smoothening of various ferrous and non-ferrous parts. LP achieves good surface finishing without deteriorating the overall structural form. This occurs by melting and redistributing a thin layer of molten material over the surface. The surface tension of the molten material attempts to minimize the surface energy induced by capillary action or temperature gradients. Since no material removal takes place, the overall form of the geometric feature is preserved. In more general terms, LP opens new avenues in cost effective manufacturing of value-added parts, components and tooling with complex 3D geometry. This happens through the elimination of manual or other types of finishing operations. This will significantly reduce the overall tooling cost (up to 40%) and manufacturing time (up to 30%). The efficiency of LP technology was already proven since improvements of the surface quality as high as ~90% (from S_a = 1.35 um before to S_a = 0.18 um after LP, respectively) were already demonstrated [7]. LP of AM parts proved to be viable in fabrication of denture implants and

dentures that require smooth surfaces to prevent bacteria build up [8]

The main objective of this study was to identify and characterize AM parts surface quality evolution with respect to powder flow orientation during the DLD process. Secondly, the transformation of surface quality between pre- and post-LP DLD parts was compared in detail by means of overall surface quality (CS_aW_a) as well as spatial frequency domain specific surface characteristics surface roughness (S_a) and surface waviness (W_a).

2. Direct laser deposition as an advanced AM process

Direct laser deposition (DLD) is one of the additive manufacturing (AM) technologies developed in mid-1990s at the National Research Council of Canada (London, ON, Canada). The process is based on a laser cladding technology and produces net-shape 3D-geometries through a layer-by-layer deposition of molten-and-solidified powder [9-11]. The schematics of a three-axis DLD process is shown in Fig. 1. This experimental setup was conceived as a complex opto-electro-mechanical system integrating a 1 KW pulsed Nd:YAG laser, laser beam focusing optics, precision powder feeder, multi-axis motion platform, and PC-based CNC control.

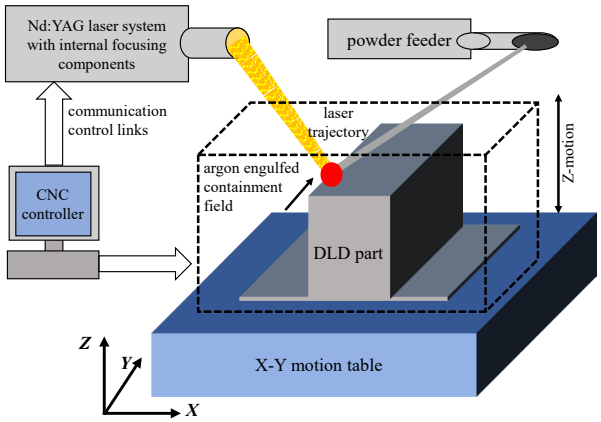

Fig. 1 Schematics of DLD system (adapted from [9,10].

During the DLD process, a CAD model of the desired geometry is taken as an input for generating layer-by-layer laser beam path trajectory. CNC software controls and synchronizes multi-axis motions of a laser focused beam as well as the precision deposition of blown powder that is rapidly melted and solidified by the laser energy. The laser-material interaction zone is located into an Argon-filled environment with a low oxygen level (typically < 50 ppm) preventing oxidation. This setup enables the fabrication of the precise functional geometries with intricate shape that are difficult or even impossible to fabricate through conventional manufacturing processes [9-11].

3. Surface topology characterization of DLD samples

The main advantage of the DLD process is represented by the generation of free-of-cracks parts with fine microstructures induced by rapid directional melting and solidification process. Therefore, DLD process development and optimization requires metallurgical evaluation and mechanical testing [9-11]. However, in this case, selection and optimization of the DLD process parameters will be required for each material and alloy. As an example, extensive investigations of the metallurgical and physical-mechanical properties of the DLD parts from nickel–chromium–cobalt superalloy IN-738 were performed [11]. IN-738 is one of most suitable alloys for hot section turbine airfoils and for hot corrosion-prone applications exhibiting excellent creep strength and hot corrosion resistance. For such extensive studies, specially designed 12 mm square tubular thin-walled samples were DLD using spherically shaped gas-atomized IN-738 alloy powder ranging from 15 µm to 45 µm in diameter (Fig. 2). These samples were used in this study during the investigation of the surface quality characteristics.

Fig. 2 DLD-fabricated tubular thin wall sample.

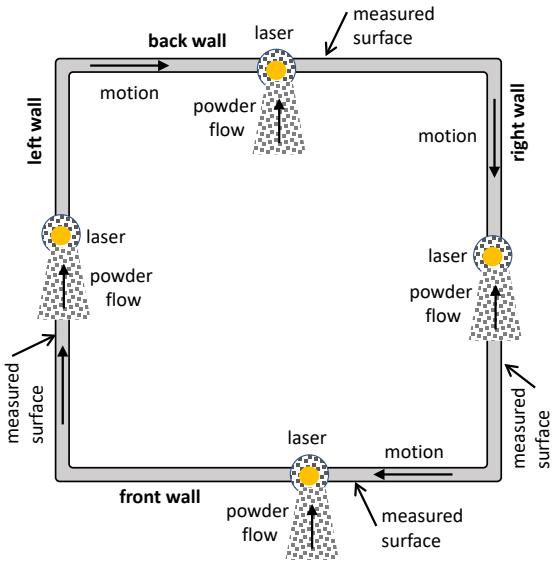

Fig. 3 Schematics of the DLP process kinematics with respect to powder flow-motion orientation and formation of walls and their surface topography.

As the sample was created by a single-feed three-axis DLD process, it opened a unique opportunity to investigate the effect of the DLD process configuration during forming each wall (front, back, left, right) and corresponding surface quality characteristics. In this particular DLD variant, each wall of the tubular sample was formed by different process configuration with respect to the powder feed nozzle orientation relative to the build-up direction/laser beam path trajectory direction. As shown in Fig. 3, four different DLD process configurations are possible: a) front orthogonal

while forming the front wall; here, the nozzle is oriented perpendicular to the travel trajectory and powder is blown to the outer surface of the wall, b) back orthogonal while forming the rear wall; here, the powder is blown to the inner surface of the wall, c) down-feed configuration while forming the left wall; here, the powder is blown along the laser path trajectory, essentially by trailing the laser beam and d) up-feed configuration while forming the right wall; here, the powder is blown along the laser path trajectory but against it. It is obvious that for each of the four walls, the relative orientation between laser motion and powder delivery direction changes. Therefore, the surface topography on each of the four walls of the sample is formed differently thus resulting in dissimilar surface quality characteristics of the surface topography.

The surface topographies of the samples were measured by means of a WYKO NT1100 optical profilometer characterized by 1 Å measurement resolution. The profilometer was set to have an areal resolution of 1.29 µm along the X- and Y-axes. For the present study, the vertical scanning interferometry mode was utilized. This enables measurement of surface textures of up to several millimeters high. To expand the measuring envelope, the profilometer's auto-stitching option was also applied. This involves a series of overlapping measurements, after which best fit was used to merge all separate patches into one large surface.

Next, ASME B46.1, ISO 4288 and ISO 11562 standards were used during surface topography analysis. According to ISO 4288, a scanning length (equaling to a cut-off length) of $\lambda_c = 2.5$ mm is recommended for an expected combined areal average surface roughness and waviness (CS_aW_a) range of 2–10 µm. Three adjacent sub-areas were taken encompassing a total measurement length of ~8 mm for each surface texture measurement. Samples of typical surface topographies for each of the four representative walls and their LP surfaces are presented in Fig. 5.

Quality characteristics of measured topographies were calculated by means of the methodology presented in [12]. Initially, the CS_aW_a calculated within a wavelength range of 5.2-5324.8 µm as a lateral X-Y resolution of a measured topography was found to be 1.29 µm. After that, a cutoff wavelength of 2.5 mm was used to separate an areal average surface roughness S_a within 5.2-2662.4 µm wavelength range and waviness W_a within 2662.4-5324.8 µm wavelength range. The results are summarized in Table 1.

Table 1 Surface characteristics of DLD sample walls

	front	left	right	back
CS_aW_a (5.2-5,324.8 µm), µm	3.510	4.418	3.903	7.758
S_a (5.2-2,622.4 µm), µm	0.704	1.781	1.766	3.861
W_a (2,622.4-5,324.8 µm), µm	2.806	2.638	2.173	3.897

These results demonstrate that the actual surface quality of the DLD sample varies significantly depending on the DLD process configuration as represented by the relative orientation of the powder delivery nozzle with respect to the laser beam path trajectory. The best surface quality was obtained for the front wall that was characterized by minimal values of $CS_aW_a = 3.510$ µm, $S_a = 0.704$ µm, and $W_a = 2.806$ µm. This is most likely a consequence of the fact that the focused laser beam fully covers the powder stream and thus melts most of the particles. In this case, there is a minimum volume of unmelted powder particles in the laser-powder interaction area. Therefore, the surface quality of the DLD wall was mainly determined by the rapid melting and solidification processes.

When the configuration of the DLD process was changed for the left and right walls, the powder was blown down (behind) and up (against) the trajectory of the laser beam, such that only a portion of the powder stream was covered by the laser spot. As such, some loose unmelted powder particles tend to be redeposited on the walls behind the laser beam. This increases CS_aW_a by 11.2% (from 3.510 µm to 3.903 µm) for the right wall and by 25.9% for the left wall. The lowest surface quality was present on the rear wall ($CS_aW_a = 7.758$ µm, $S_a = 3.861$ µm, and $W_a = 3.897$ µm), values that were increased by 121.0%, 38.9%, and 448.6%, respectively (with respect to the front wall). These results were predictable since the DLD process configuration for the rear wall has an opposing trajectory-powder flow orientation (-90°) with respect to the configuration used for the front wall.

In addition to the overall analysis of the surface quality in terms of areal average roughness and waviness, it is also important to understand the particular components of the surface topography. This information can be critical in the determination of the main sources contributing to the formation of the surface topography. One of the wide applications of this approach is represented by the calculation of the surface topography spectrum before and after LP process. This is required to determine the effectiveness and applicability of the LP process towards the improvement of the surface quality [2-4, 12]. This approach also allows to identify most suitable initial surface topography for the achievement of the best possible final surface quality.

The surface topography spectrum calculated for each wall of the DLD sample is shown in Fig. 4. The waviness component within 2662.4-5324.8 µm was already discussed above since it follows the trend of surface quality reduction: from the best quality associated with the front wall, lower for the left and right walls and further reduced for the rear wall. With respect to the areal average waviness, areal average roughness encompasses a more comprehensive amount of information since it includes significantly more wavelength ranges. These intervals cover everything from the four intervals of the spatial resolution associated with the lowest possible measured wave and up to a cutoff wavelength of 2.5 mm, as defined by the measured CS_aW_a in ISO 4288.

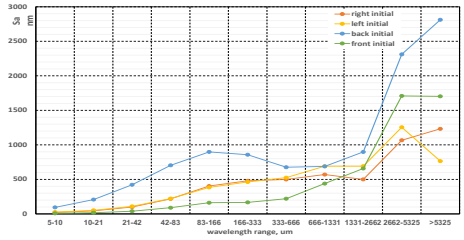

Fig. 4 Surface topography spectrums of DLD sample walls.

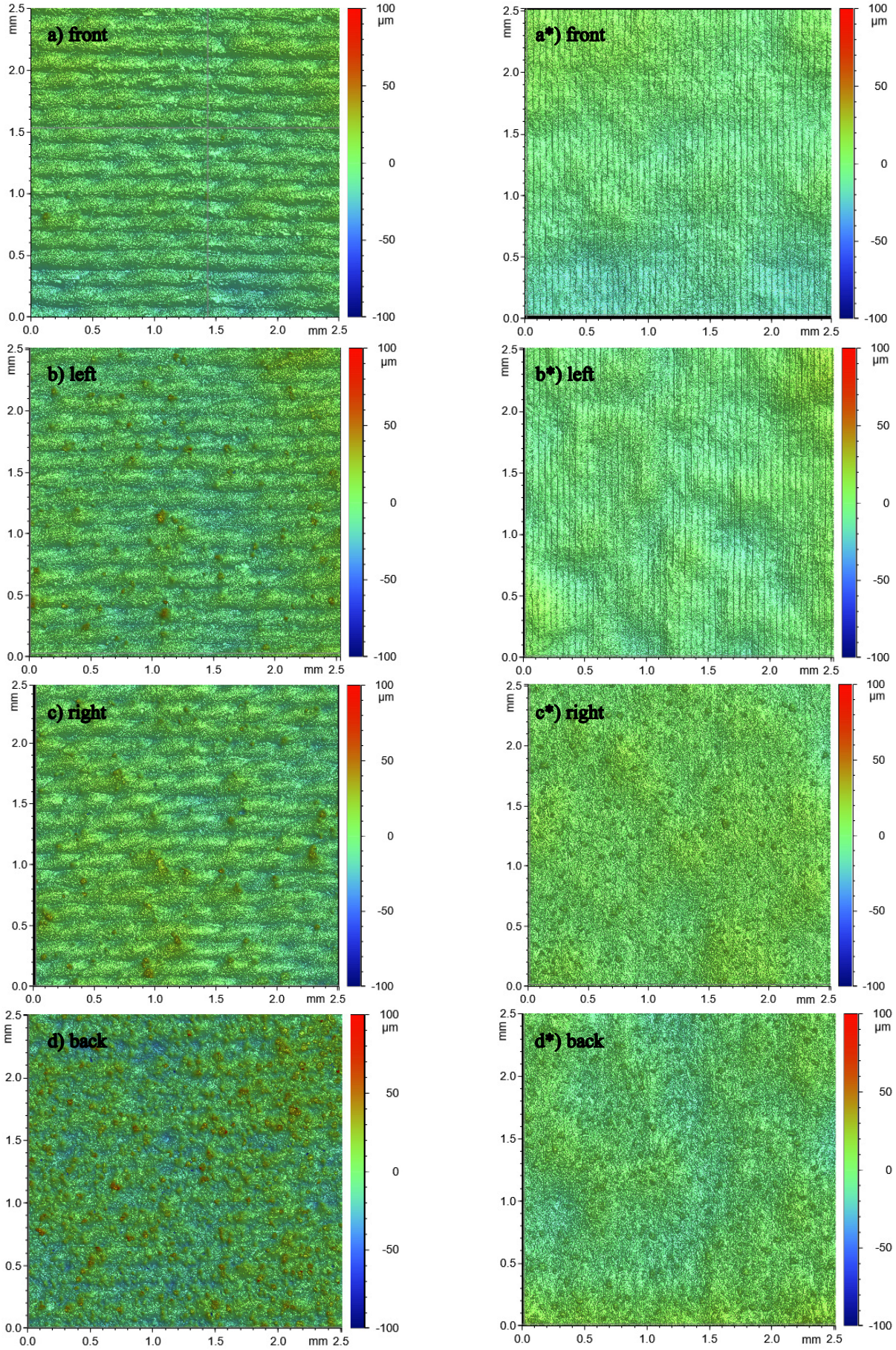

Fig 5: Typical surface topographies of the post- and pre-LP-DLD sample walls: a) front, b) back, c) left, and d) right (the asterisk denotes the LP-DLD surface).

Typically, DLD process uses powder particles having a diameter of 15-45 μm [10]. This is why an average roughness within a low-wavelength range of 5.2-41.6 μm and middle-wavelength range of 41.6-332.8 μm is significantly higher (e.g., by 699.6% for 83.2-166.4 μm range) than for a high-wavelength range of 332.8-2662.4 μm (e.g. by 156.2% for 332.8-665.6 μm range) with respect to the front wall. These significant differences in areal surface roughness components are caused by the inconsistencies in DLD process configuration leading to higher instabilities in laser-powder interactions and in melting-solidification process.

4. Laser polishing as an advanced finishing process

Laser polishing (LP) is a novel advanced rapid post processing technology used to transform rough, low-quality surfaces to high-quality/high-gloss surfaces. As stated previously, LP can produce high quality surfaces up to 30% faster than traditional abrasive and chemical polishing. LP relies on a laser beam that brings a superficial layer of initial surface topography (peaks and valleys) to a molten state. As the laser beam travels along its trajectory, molten pool develops according to several thermodynamic phenomena (capillary action, gravitational force, and thermocapillary action involving surface tension gradients induced by high temperature gradients). Molten pool dissipates heat through radiation and convection to the surrounding air and through conduction to bulk material (Fig. 6). The newly formed topography exhibits less variations because surface micropeaks are melted and fill in the microvalleys thus ultimately lowering the amplitude of spatial topography. This can be used to classify LP as a spatial frequency filter that minimizes the small sporadic variation (high spatial frequency structures or S_a) and preserves the larger longer spatial structures (low spatial frequency structures or W_a). One of the reasons for the conservation of these structures is related to the undersized beam diameter compared to the size of the structures being polished. As such, it is possible to analyze the post-LP DLD surfaces by separating the two spatial frequency ranges (S_a and W_a).

The system used to conduct LP involves three individual sub-systems that are synergistically integrated to provide reliable, precise, and accurate LP: optoelectrical laser beam delivery system, CNC stages, and computer control. The laser beam delivery system includes a beam collimator, optical mirrors with angular displacement ability, objective lens for focusing of the beam and *f*-theta lens with a focal length of 160 mm. The laser used was Nd:YAG 1070 nm, 500 W continuous wave laser. The laser system was affixed to the Z CNC-controlled stage for vertical translation. The workpiece was attached to the XY CNC stage for translations in the horizontal plane. Much like the DLD process, LP process is performed in an argon-rich controlled environment capable to prevent the oxidation of the polished surface. Lastly, the communication subsystem controls the precise movements of the XYZ stage (0.1 μm) as well as the movement of the optical mirrors within the laser subsystem. Fig. 7 presents a schematic of the LP system. A power of less than 100 W and speed of 100 mm/s was used to conduct a one-pass polish of the investigated areas.

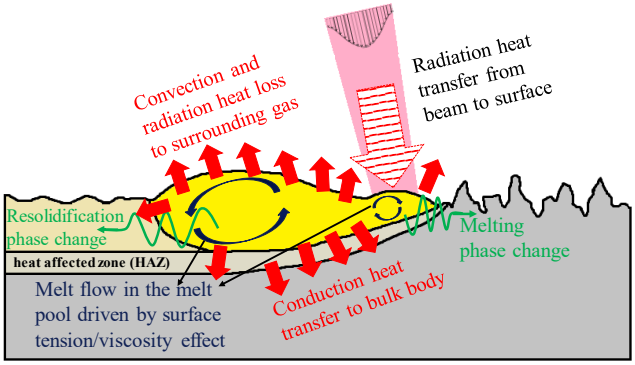

Fig. 6 Demonstration of the reallocation and resolidification of the molten-state metal during laser polishing.

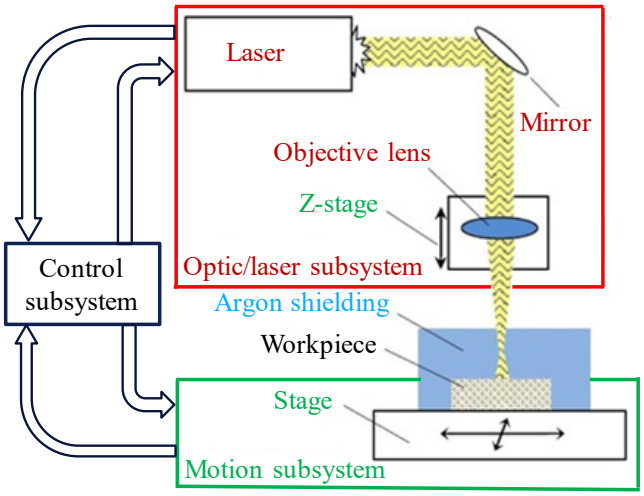

Fig. 7 Schematic of the laser polishing system.

5. Topology characterization of DLD-LP samples

As shown above, DLD-generated surfaces lead to variable surface topographies dependent on the orientation of the powder-feed nozzle relative to the laser delivery location. More specifically, the front wall is associated with the highest quality of the post-LP surface due to the 90º orientation of the powder feed nozzle relative to the laser beam feed. By contrast, the -90º relative positioning used for the rear wall leads to the roughest post-LP surface. Nonetheless, even though the front wall has the best surface quality, its roughness might be regarded as insufficiently low for certain applications. Therefore, to remain in sync with the high productivity of DLD, this technology has to be followed by another high-speed finishing technique such as LP (Fig. 8). As such, it is of upmost importance to investigate the the effect of LP on DLD-formed structures.

LP could be regarded as a low spatial frequency S_a filter applied on surfaces created through subtractive machining procedures. Based on this, it could be assumed that LP would act in the same manner on DLD-fabricated surfaces. Along these lines, Fig. 9 illustrates the changes occurred after LP was performed on DLD parts. By relying on criteria similar to those used during the characterization of DLD parts, S_a ranges from wavelengths of 5.2 – 2662.2 μm and spatial wavelength range from 2662.4 μm – 5325.8 μm is considered as W_a.

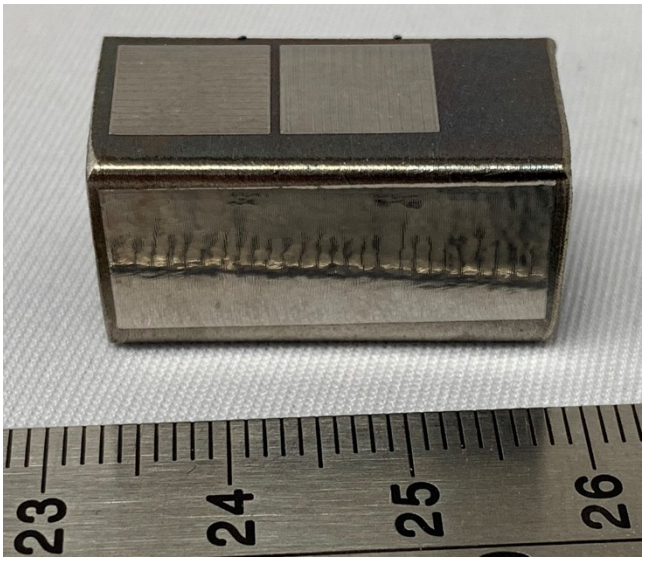

Fig. 8 DLD-LP sample

Table 2 Surface characteristics of DLD-LP sample walls

	front	left	right	back
CS_aW_a (5.2-5,324.8 µm), µm	3.563	3.223	2.923	3.853
S_a (5.2-2,622.4 µm), µm	0.211	0.521	0.423	0.444
W_a (2,622.4-5,324.8 µm), µm	3.352	2.702	2.500	3.408

Table 3 Improvement of the surface characteristics of DLD-LP sample walls with respect to the DLD sample

	front	left	right	back
CS_aW_a (5.2-5,324.8 µm), %	-1.5	27.1	25.1	50.3
S_a (5.2-2,622.4 µm), %	70.0	70.7	76.1	88.5
W_a (2,622.4-5,324.8 µm), %	-19.5	-2.4	-17.0	12.5

As seen from Tables 2 and 3, LP conducted on all four DLD formed walls had an improvement of over 70%. The most noticeable improvement occurred on the rear wall that had an initial S_a of 3.861 µm that was reduced to 0.444 µm by means of LP (88.5% improvement).

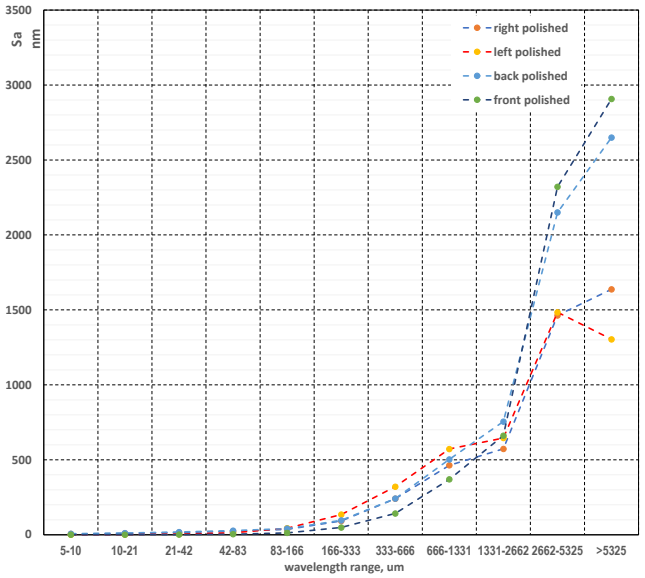

Fig. 9 Topography spectrum of LP-DLD walls.

It is also to be noted that S_a decreases relatively at the same rate for all four walls. By contrast, W_a was not affected by the LP since the beam in unable to melt structures that are larger than the size of the laser spot diameter. Thus, post-LP DLD-formed surfaces may still encompass large particles or large step-like structures. Further investigations will have to determine LP parameters capable to ensure the highest possible post-polished surface quality.

6. Summary and conclusions

The present study examined the viability of LP as a finishing technique to be used on DLD-generated surfaces. The analysis performed was focused on the characterization of the surface quality performed through the spectrum of the spatial frequencies. The same analysis was also conducted on the post-LP DLD-generated surfaces. Several conclusions can be drawn as a result of this work:

- DLD is a superior procedure for rapid manufacturing of parts due to its ability to form and create 3D freeform geometries in a rapid fashion. DLD relies on the melting of the metallic particles comprising the powder by means of laser energy. During solidification, molten particles fuse together and form the DLD surface.
- The variable relative orientation between the powder-fed nozzle and the laser feed direction leads to a variable surface quality of the DLD-generated surface. More specifically, when the powder-nozzle is orientated at 90º with respect to the laser feed direction (*i.e.*, the powder is fed in front of the laser) the particles melt in full and fuse with the previous layer. This orientation results in a S_a of 0.740 µm and a CS_aW_a of 3.510 µm. Contrastingly, when the orientation is -90º (powder is fed orthogonally to the laser beam trajectory towards the inner wall) the surface roughness is the worst since the powder metal continues to be added to the molten pool even though the solidification has already started. This leads to the presence of solid powder particles within the DLD-formed surface and this in turn contributes to a relatively rough surface (S_a = 3.861 µm and CS_aW_a = 7.758 µm).
- LP's low spatial frequency filter functionality is a practical solution for expediting the post-processing of rough parts. Since the DLD-generated surfaces are or can be very rough, LP could be used to post-process DLD parts in order to improve their surface quality and thereby meet the high-quality criteria set by consumer applications. When LP was used on front and rear walls, the S_a dropped to 0.211 µm and 0.444 µm respectively. These 70 % and 88.5% improvements imply that LP can be used to elevate the quality of DLD surfaces in a fast and efficient manner.
- Since DLD and LP are or can be automated, both processes can incorporate elements of artificial intelligence (AI) for superior adaptive control, self-optimization, and online monitoring. The addition of AI would enable a more reliable DLD-LP process by allowing computer vision to direct alterations of the process parameters that are meant to ensure that the powder is optimally fed with respect to laser feed direction as well as that laser settings are optimized for the achievement of the highest possible surface quality.

Acknowledgments

This study is the result of collaboration between the National Research Council of Canada (London, Ontario) and Western University (London, Ontario). Partial financial support was also provided by the Natural Sciences and Engineering Research Council (NSERC) of Canada.

References

[1] H. Hassanin, A. Elshaer, R. Benhadj-Djilali, F. Modica, and I. Fassi: "Micro and Precision Manufacturing" ed. by K. Gupta, (Springer, Cham, 2018) p.145.
[2] E. Willenborg: Dissertation RWTH Aachen, (Shaker Verlag, Aachen, 2006)
[3] E. Willenborg: "Tailored Light 2: Laser Application Technology" ed. by R. Poprawe, (Springer-Verlag, Berlin Heidelberg, 2011) p.196.
[4] A. Temmler, E. Willenborg, and K. Wissenbach, Proc. SPIE, 8243, (2012) 82430W.
[5] F.E. Pfefferkorn, N.A. Duffie, X. Li, M. Vadali, and C. Ma: CIRP Ann. Manuf. Technol., 62, (2013) 203.
[6] E.V. Bordatchev, A.M.K. Hafiz, and O.R. Tutunea-Fatan: Int. J. Adv. Manuf. Technol., 73, (2014) 35.
[7] A.M.K. Hafiz, E.V. Bordatchev, and R.O. Tutunea-Fatan: J. Manuf. Process., 14, (2012) 425.
[8] G. Annamaria, B. Massimiliano, and V. Francesco: Int. J. Adv. Manuf. Technol., 120, (2022) 1433.
[9] L. Xue and M. Islam: J. Laser Appl., 12, (2000) 160.
[10] L. Xue, J. Chen, and S.H. Wang: Metallogr. Microstruct. Anal., 2, (2013) 67.
[11] J. Chen and L. Xue: Mater. Sci. Eng. A, 527, (2010) 7318.
[12] E.V. Bordatchev and A.M.K. Hafiz: Meas. Sci. Technol., 25, (2014) 095601

(Received: June 6, 2022, Accepted: January 19, 2023)